



Published in final edited form as:

Hepatology. 2014 April ; 59(4): 1351–1365. doi:10.1002/hep.26938.

Liver-primed CD8⁺ T cells suppress antiviral adaptive immunity through Gal-9-independent Tim-3 engagement of HMGB-1 in mice

Joseph S. Dolina¹, Thomas J. Braciale^{1,2}, and Young S. Hahn^{1,2}

¹Department of Microbiology, Immunology, and Cancer Biology, Beirne B. Carter Center for Immunology Research, University of Virginia, Charlottesville, VA 22908

²Department of Pathology, University of Virginia, Charlottesville, VA, 22908

Abstract

The liver is a tolerogenic environment exploited by persistent infections such as hepatitis B (HBV) and C (HCV) viruses. In a murine model of intravenous (IV) hepatotropic adenovirus infection, liver-primed antiviral CD8⁺ T cells fail to produce pro-inflammatory cytokines and do not display cytolytic activity characteristic of effector CD8⁺ T cells generated by infection at an extrahepatic, *i.e.* subcutaneous (SC), site. Importantly, liver-generated CD8⁺ T cells also appear to have a T regulatory (T_{reg}) cell function exemplified by their ability to limit proliferation of antigen-specific T effector (T_{eff}) cells *in vitro* and *in vivo* via Tim-3 expressed by the CD8⁺ T_{reg} cells. Regulatory activity did not require recognition of the canonical Tim-3 ligand Gal-9 but was dependent on CD8⁺ T_{reg} cell surface Tim-3 binding to the alarmin HMGB-1. Conclusion: virus-specific Tim-3⁺CD8⁺ T cells operating through HMGB-1 recognition in the setting of acute and chronic viral infections of the liver may act to dampen hepatic T cell responses in the liver microenvironment and as a consequence limit immune mediated tissue injury or promote the establishment of persistent infections.

Keywords

immunoregulation; intrahepatic; T_{reg}; adenovirus; cytomegalovirus

Immune cells within the liver are maintained in a state of active tolerance due to continuous exposure to microbe-derived pathogen associated molecular patterns (PAMP), toxins, and food-derived antigens (1). Hepatotropic viruses adapted to persist in the liver have evolved to take advantage of this environment and trigger dysfunctional adaptive immune responses during acute (adenovirus) and chronic (HBV and HCV) virus infections of the liver (2,3). The generation of antiviral CD8⁺ T_{eff} cells is suboptimal in the liver in part due to defective antigen presentation and a skewed CD4⁺ T_H1/T_H2 cell balance resulting in diminished T cell proliferation, decreased production of pro-inflammatory cytokines, and reduced expression of cytolytic effector molecules (4). Understanding the mechanisms that orchestrate liver tolerance is critical for antiviral immunotherapy target selection and development.

Another factor limiting intrahepatic CD8⁺ T cell responses to infection is the generation of T_{reg} cells (5). T_{reg} cells suppress T_{eff} cell responses through a variety of antigen-specific cell

Corresponding Author: Young S. Hahn, Beirne B. Carter Center for Immunology Research, University of Virginia, P.O. Box 801386, Charlottesville, VA 22908, Telephone: 434-924-1155, Fax: 434-924-1221, ysh5e@virginia.edu.

The authors declared no conflict of interest.

contact dependent/independent mechanisms including IL-2 sequestration, release of anti-inflammatory cytokines (IL-10 and TGF- β) (5), CTLA-4 co-stimulation (6), Fas/FasL or perforin killing (7,8), granzyme B (GrB) negative feedback (9), and PD-1/PD-L1 signaling (10). Notably, intrahepatic CD8⁺ T cells responding to acute and chronic HCV infections are capable of producing IL-10 and co-express PD-1/PD-L1 and Tim-3. Compelling evidence suggests that simultaneous blockade of these regulatory elements improves intrahepatic immunity prompting the development of novel therapeutics (11,12). CD8⁺ T cell derived IL-10 appears to reduce IL-12R, IL-2, IFN- γ , and Tbet expression through an autocrine mechanism (13). Programmed death 1 (PD-1), upon engagement with PD-1 ligand (PD-L1), suppresses CD8⁺ T cell responses via direct SHP-2-mediated dephosphorylation events and modulation of Ca⁺⁺ fluxes downstream of T cell receptor (TCR) signaling (14). Furthermore, Gal-9 is abundant in the liver, is induced during viral infection by IFN- γ , and upon engagement of T cell immunoglobulin and mucin 3 (Tim-3) dampens CD8⁺ T cell IL-2, IFN- γ , and proliferation (15). Gal-9 recognizes N- and O-linked glycosylation sites of the Tim-3 mucin region. However, *E. coli*-derived recombinant Tim-3 tetramers, inherently lacking oligosaccharides, can bind to B cells, T cells, dendritic cells (DC), and macrophages, suggesting other non-Gal-9 ligands for Tim-3 exist (16).

High-mobility group box 1 (HMGB-1) was recently discovered to bind the FG cleft in the immunoglobulin variable region of Tim-3 within DC endosomes (17). HMGB-1, originally identified as a DNA binding protein, is classified under the alarmins, which relay danger associated molecular pattern (DAMP) signals to antigen presenting cells (APC). Although passively released by necrotic cells, active secretion of HMGB-1 from monocytes, macrophages, DCs, and NK cells has been observed (18). Upon binding the receptor for advanced glycation end products (RAGE) expressed by DCs and T cells, HMGB-1 can directly stimulate DC maturation and T cell proliferation (19,20).

During an analysis of CD8⁺ T cell responses following infection with hepatotropic adenovirus, we hypothesized that antiviral intrahepatic CD8⁺ T cells had T_{reg} cell properties likely dependent on production of IL-10, display of Gal-9, and/or expression of PD-L1. However, we observed that the PD-1/PD-L1⁺Tim-3⁺CD8⁺ T cells did not produce Gal-9; moreover, administration of blocking antibodies to IL-10, PD-L1, and Gal-9 indicated that CD8⁺ T_{reg} cell suppression was not dependent on these mechanisms. Surprisingly, we found that Tim-3 displayed on the surface of intrahepatic CD8⁺ T_{reg} cells sequesters HMGB-1 thereby limiting augmentation of CD8⁺ T_{eff} cell proliferation. The capture of HMGB-1 by Tim-3 on the surface of CD8⁺ T_{reg} cells offers an attractive explanation for the inability of CD8⁺ T_{eff} cells to generate efficient antiviral responses in the liver.

MATERIALS AND METHODS

Animals and Infections

Thy1.2^{+/+}, *Thy1.1^{+/-}*OT-I(*Tcra/Tcrb*)^{+/-} (Taconic Farms, Hudson, NY), and IL-10 transcriptional reporter (Vert-X) mice provided by Christopher Karp (University of Cincinnati College of Medicine, Cincinnati, OH) were used in these experiments. Animals were 6 to 10 weeks of age and housed in a pathogen-free facility under protocols approved by the Institutional Animal Care and Use Committee at the University of Virginia (Charlottesville, VA).

Replication-deficient type 5 adenoviruses expressing ovalbumin (Ad-Ova) and β -galactosidase (Ad-LacZ) were provided by Timothy L. Ratliff (University of Iowa, Iowa City, IA) and Gregory A. Helm (University of Virginia), respectively. Mouse cytomegalovirus expressing ovalbumin (MCMV-Ova) was provided by Ann B. Hill (Oregon Health and Science University, Portland, Oregon). Mice were infected with 2.5×10^7

infectious units (IU) Ad-Ova/LacZ or 1×10^4 IU MCMV-Ova via intravenous (IV) injection in the caudal vein or subcutaneous (SC) injection in the left flank.

Quantitative PCR

Total RNA was isolated using the Trizol method (Invitrogen, Carlsbad, CA) and reverse-transcribed using High Capacity RNA-to-cDNA Master Mix (Applied Biosystems, Foster City, CA). Q-PCR was performed using Fast SYBR Green Master Mix (Applied Biosystems) on an AB StepOne Plus Real-Time PCR System. QuantiTect primers for *Mus musculus* *Il10*, *Il2*, *Ifng*, *Tgfb*, *Lgals9*, *Havcr2*, *Pd1*, *Pdc1*, *Ctla4*, *Klrc1*, *Foxp3*, *Irf2* (Qiagen, Valencia, CA), and self-designed primers for *Mus musculus* hypoxanthine phosphoribosyltransferase (*Hprt1*; forward, 5'-CTCCGCCGGCTTCCTCCTCA-3'; reverse, 5'-ACCTGGTTCATCATCGCTAATC-3') were used for detection.

ELISA

IL-2, IL-10, and IFN- γ ELISAs were performed according to the manufacturer's instructions (BD Biosciences, Franklin Lakes, NJ). Absorbance was read at 450 nm using a PowerWave XS Microplate Spectrophotometer (BioTek, Winooski, VT).

Immunoprecipitation and Western Blot

5 μ g of recombinant mouse Tim-3 human IgG₁ chimeric protein (rTim-3Fc) (R&D Systems, Minneapolis, MN) was added to 500 μ L supernatant and immunoprecipitated with Protein A/G PLUS-Agarose (Santa Cruz Biotechnology, Dallas, TX). Proteins were resolved, western blotted, and incubated with rabbit anti-HMG1/2/3 (pAb) (Santa Cruz Biotechnology), biotinylated anti-human IgG (pAb) (SouthernBiotech, Birmingham, AL), HRP-linked anti-rabbit IgG (pAb) (Cell Signaling Technology, Danvers, MA), and streptavidin-HRP (R&D Systems) followed by visualization with SuperSignal West Pico Chemiluminescent Substrate (Thermo Scientific, Rochester, NY).

Liver and Spleen Mononuclear Cell Isolation

Mononuclear cells were isolated from livers via Histodenz (Sigma-Aldrich, St. Louis, MO) gradient centrifugation and spleens over a Ficoll (Atlanta Biologicals, Lawrenceville, GA) gradient according to previous work (2).

In Vitro Suppression Assay

Bone marrow-derived dendritic cells (BMDC) were matured for one week in RPMI Medium 1640 containing 10% HyClone fetal bovine serum, 15 mM HEPES Buffer, 50 μ M β ME, 20 ng/mL rIL-4, and 20 ng/mL rGM-CSF (eBioscience, San Diego, CA). 5×10^3 BMDCs were pulsed for 5 hrs with 10 ng/mL SIINFEKL or ICPMYARV peptides (AnaSpec, Fremont, CA), then cultured with 5×10^4 CFSE-labeled (Invitrogen) naïve Thy1.1⁺CD8⁺ OT-I T cells. CD8⁺ T cells from SC or IV infected C57BL/6 mice were then added at the appropriate ratio. CD8⁺ T cells were positively sorted using anti-CD8 α magnetic beads (Miltenyi Biotec, Auburn, CA).

In Vivo Suppression Assay

For *in vivo* liver responses, 5×10^5 CFSE-labeled naïve Thy1.1⁺CD8⁺ OT-I T cells were transferred into naïve, D7 Ad-Ova infected, or D7 Ad-LacZ infected mice prior to IV MCMV-Ova infection. For *in vivo* lymph node responses, 3×10^6 CD8⁺ T cells from SC or IV infected C57BL/6 mice were co-transferred with 1.5×10^6 CFSE-labeled naïve Thy1.1⁺CD8⁺ OT-I T cells into SC infected C57BL/6 mice at D0.

Antibody Blockade and Cell Treatments

In vivo whole animal blockade of HMGB-1, PD-L1, and Tim-3 was conducted via intraperitoneal (IP) injection of 300 µg anti-HMGB-1 (pAb) (Shino-Test Corporation, Kanagawa, Japan), anti-PD-L1 (10F.9G2), or anti-Tim-3 (RMT3-23) (BioXCell, West Lebanon, NH). For *in vitro* and *in vivo* lymph node blockade, CD8⁺ T_{reg} cells were pre-coated with 20 µg/mL anti-PD-L1 and/or anti-Tim-3 for 1 hr at 37°C. 1.0 µg/mL recombinant mouse Gal-9 (rGal-9) (R&D Systems), 20 µg/mL anti-Gal-9 (RG9-1), 20 µg/mL anti-IL-10R (1B1.3A) (BioXCell), and 0.5 µg/mL anti-HMGB-1 (pAb) (eBioscience) were added to culture media in relevant experiments.

Flow Cytometry

Antibodies from BD Biosciences, Biolegend, eBioscience, and R&D Systems were used for detection. H2-K^b Ova-tetramer APC (Baylor College of Medicine, Houston, TX) and H2-K^b βGal-tetramer PE (NIAID, Atlanta, GA) identified antigen-specific CD8⁺ T cells. 1.5×10⁶ mononuclear cells were blocked with anti-CD16/CD32 (2.4G2) (University of Virginia) followed by specific antibody labeling. Nuclear transcription factor staining was achieved using the FoxP3 Staining Set (eBioscience). For intracellular cytokine detection, cells were re-stimulated with 5 ng/mL PMA and 500 ng/mL ionomycin (Sigma-Aldrich) or 2 µg/mL SIINFEKL peptide (AnaSpec) and blocked with 1 µL/mL GolgiPlug/GolgiStop (BD Biosciences). Data were collected on a BD FACS Canto II (BD Immunocytometry Systems, San Jose, CA) and analyzed using FlowJo 8.8.6 software (Tree Star Inc., Ashland, OR). Cells were FACS-sorted on an iCyt Reflection Cell Sorter (iCyt Mission Technology, Champaign, IL).

Microscopy

Human HCC and HCV liver biopsies kindly provided by the Biorepository and Tissue Research Facility and Valeria R. Mas (University of Virginia), respectively, were fixed in chilled acetone for 2 min. Mouse tissues were flushed with 1×PBS and periodate-lysine-paraformaldehyde fixative (PLP), excised, incubated in PLP for 3 hrs at 4°C, and passed over a sucrose gradient. Tissues were frozen in OCT, sectioned at 5 µm thickness, blocked with 2.4G2 solution (2.4G2 media containing anti-CD16/32, 30% chicken/donkey/horse serum, and 0.1% NaN₃), and stained with antibodies from BioLegend, eBioscience, Santa Cruz Biotechnology, and Sino Biological. In select experiments, cells were also labeled with CFSE and Vybrant CM-DiI (Invitrogen). Confocal microscopy was performed on a Zeiss LSM-700, and data were analyzed using Zen 2009 Light Edition software (Carl Zeiss MicroImaging GmbH, Jena, Germany).

Statistical Analysis

Significant differences between experimental groups were calculated using the two-tailed Student's *t* test or one-way ANOVA (with group comparisons = 3). Data analysis was performed using Prism 5.0a software (GraphPad Software Inc., La Jolla, CA). Values of *P* < 0.05 were regarded as being statistically significant and noted as * < 0.05, ** < 0.01, and *** < 0.001.

RESULTS

Liver-primed CD8⁺ T cells exert a T_{reg} suppressor function on the priming of naïve CD8⁺ T cells *in vitro* via linked suppression

IV adenovirus infection of mice is characterized by a decrease in target cell lysis from day 7 (D7) to D14 exemplified by a drop in serum ALT. Antigen-specific CD8⁺ T cells primed directly in the liver after IV infection peak in absolute number at D7 but fail to produce

TNF- α , IFN- γ , and GrB compared to CD8⁺ T cells that have trafficked to the liver from the inguinal lymph node (Ig LN) in response to SC adenovirus inoculation (Supporting Fig. 1) (2). To expand our studies upon the potential roles of anti-inflammatory mediators utilized by liver-primed CD8⁺ T cells, we examined cellular production of IL-10 and the expression of PD-1/PD-L1 and Tim-3. After IV infection with adenovirus expressing ovalbumin (Ad-Ova), liver CD8⁺ T cells had elevated intracellular IL-10 at D7 compared to SC generated CD8⁺ T cells (Fig. 1A). The secretion of IL-10 was also detectable in culture supernatants of TCR-stimulated CD8⁺ T cells sorted from the IV infected liver (Fig. 1B). PD-1 and Tim-3 co-expression peaked at D7 (Supporting Fig. 2) and was significantly enriched on Ova Tet⁺CD8⁺ T cells in the livers of IV infected mice (Fig. 1C,D). In spite of the lower absolute number of CD8⁺ T cells infiltrating the livers and spleens of SC infected mice, the frequency of Ova-specific CD8⁺ T cells was comparable between IV and SC infections. IV infection with adenovirus expressing β -galactosidase (Ad-LacZ) yielded comparable results (Fig. 1C). Route of infection had no impact on the expression of PD-L1 in the liver. The expression of the Tim-3 ligand Gal-9 was readily detectable on naïve and SC CD8⁺ T cells, but only low expression was observed on liver-primed CD8⁺ T cells (Fig. 1E).

Since IL-10-producing, PD-1/PD-L1⁺Tim-3⁺CD8⁺ T cells appeared at a late time point post-adenovirus infection (D7), we hypothesized that liver-primed CD8⁺ T cells, rather than acting as effector cells, contribute to limiting local inflammatory responses by suppressing T_{eff} cells migrating to the hepatic microenvironment. To test this, we utilized an *in vitro* system employing TCR transgenic OT-I T cells, where Thy1 congenically mismatched CFSE-labeled naïve CD8⁺ OT-I T cells were placed in co-culture with CD8⁺ T cells isolated from the infected D7 SC spleens or IV livers. BMDCs pulsed with ovalbumin octapeptide (Ova₂₅₇₋₂₆₄:SIINFEKL) served as the APC. CD8⁺ T cells isolated from the D7 livers of IV adenovirus infected mice had markedly suppressed OT-I T cell proliferative expansion by D2 to D3 of culture as evident from the absolute number and division index of dividing OT-I T cells, while CD8⁺ T cells isolated from the D7 SC spleens had no suppressive effect (Fig. 2A,B). Suppression was observed over a range of OT-I:IV CD8⁺ T ratios (Fig. 2C). Significantly less IL-2 and IFN- γ could be detected in the supernatants collected from OT-I/IV CD8⁺ T cell co-cultures (Fig. 2D) along with diminished CD25 expression on OT-I T cells exposed to liver-primed CD8⁺ T cells (Fig. 2E). The regulatory activity mediated by these liver-primed CD8⁺ T_{reg} cells was also dependent on TCR recognition of specific antigen (Supporting Fig. 3), suggesting liver-primed CD8⁺ T_{reg} cells mediate suppression in an antigen-specific manner. Liver-primed CD8⁺ T_{reg} cells did not appear to induce cell death in responder OT-I T cells (Supporting Fig. 4).

Cellular markers and properties associated with liver-primed CD8⁺ T_{reg} cells

Hallmarks of CD4⁺ T_{reg} cells include FoxP3 and CD25 expression, lack of IL-2 production, and failure to undergo robust clonal expansion following TCR/antigen exposure. We analyzed a panel of markers and found that the intrahepatic Ova Tet⁺CD8⁺ T_{reg} cells had markedly diminished *Il2* mRNA, lacked enhanced *Foxp3* mRNA, but maintained elevated levels of *Il10*, *Havcr2* (Tim-3), *Pdcl* (PD-1), and *Ikgf2* (Helios) mRNA compared to Ova Tet⁺CD8⁺ T cells (Fig. 3A). Intracellular Helios and cell surface GITR was expressed by the Ova Tet⁺CD8⁺ T_{reg} cells, but surface CD25 and surface/intracellular CTLA-4 was not detectable (Fig. 3B). It has been reported that expression of inhibitory Ly49 receptors along with restriction of Qa-1 recognition define a subset of CD8⁺ T_{reg} cells (8). We could not detect surface expression of Ly49 receptors on these liver CD8⁺ T cells, but low-level expression of NKG2A and Qa-1 was detected (Fig. 3B; data not shown, respectively).

To explore the role of IL-10, we infected IL-10 transcriptional reporter eGFP expressing (Vert-X) mice with Ad-Ova and FACS-sorted eGFP⁺ and eGFP⁻CD8⁺ T cells from the D7

liver. eGFP⁺CD8⁺ T cells maintained elevated *Havcr2*, *Pdc1*, and *Irf2* mRNA compared to eGFP⁻CD8⁺ T cells (Fig. 3C), and eGFP expression positively correlated with PD-1 and Tim-3 expression (Fig. 3D). Given these observations, we explored the IL-10 pathway and other regulatory mechanisms (e.g. PD-1/PD-L1 and Tim-3) to account for the suppressive activity of the liver-primed CD8⁺ T_{reg} cells.

CD8⁺ T_{reg} cells suppress T_{eff} cells in a Tim-3-dependent manner

When we compared the suppressive activity of liver eGFP⁺ and eGFP⁻CD8⁺ T_{reg} cells we found that eGFP⁺CD8⁺ T_{reg} cells were more effective at suppressing OT-I T cell division *in vitro* (Fig. 3E) presumably due to IL-10 secretion and possibly elevated expression of the regulatory molecules PD-1/PD-L1 and Tim-3. However, anti-IL-10R antibody could not reverse suppression (Fig. 3F). These data indicate that IL-10 phenotypically marks the CD8⁺ T_{reg} cell but does not have a central role in suppression.

CD8⁺ T_{reg} cells were then pre-coated with anti-PD-L1, anti-Tim-3, or both antibodies. Anti-PD-L1 antibody had no effect, but anti-Tim-3 antibody partially rescued OT-I T cell division (Fig. 4A,B). Tim-3 blockade also resulted in enhanced release of IL-2 and IFN- γ into the supernatants collected from OT-I/IV CD8⁺ T_{reg} cell co-cultures (Fig. 4C). Thus, Tim-3 blockade appeared to inhibit CD8⁺ T_{reg} cell ability to suppress CD8⁺ T_{eff} cells.

Nascent CD8⁺ T cell expansion during liver and lymph node antiviral responses is suppressed by liver-primed CD8⁺ T_{reg} cells *in vivo*

We next examined whether liver-primed CD8⁺ T_{reg} cells could regulate the expansion of endogenous CD8⁺ T_{eff} cells *in vivo*. To this end, naïve, Ad-Ova, or Ad-LacZ infected mice were re-infected with mouse cytomegalovirus expressing ovalbumin (MCMV-Ova) at D7 post-adenovirus infection, and D14 livers were analyzed. Seven days following MCMV-Ova infection, the absolute number of viable mononuclear cells in the livers of mice previously immunized with Ad-Ova was reduced compared to Ad-LacZ infected, MCMV-Ova challenged animals (Fig. 5A). Further, animals undergoing initial Ad-Ova infection had reduced frequencies of IFN- γ ⁺ and TNF- α ⁺IFN- γ ⁺ antigen-specific CD8⁺ T cells (Fig. 5B). These results support and reinforce our *in vitro* data and implicate CD8⁺ T_{reg} cells within the infected liver as the mediators of suppression operating in an antigen-specific manner.

To further demonstrate the *in vivo* suppressive effect of CD8⁺ T_{reg} cells, Thy1.1⁺CD8⁺ OT-I T cells were adoptively transferred into naïve and D7 Ad-Ova infected mice prior to MCMV-Ova infection. The numbers of Thy1.1⁺CD8⁺ OT-I T cells in the livers of mice previously infected with Ad-Ova were reduced but were partially recovered via IP delivery of anti-Tim-3 antibody at D5 and D6 (Fig. 5C). No improvements in the frequencies of IFN- γ ⁺ and TNF- α ⁺IFN- γ ⁺ antigen-specific CD8⁺ T cells were observed (Fig. 5D). These observations support the concepts that the regulatory effect of CD8⁺ T_{reg} cells is antigen-specific and that Tim-3 plays an important role in mediating suppression.

To more directly demonstrate the immunoregulatory effect of liver-primed CD8⁺ T_{reg} cells on antigen-specific CD8⁺ T_{eff} cell responses *in vivo*, D7 Ad-Ova SC splenic CD8⁺ T cells, D7 IV liver CD8⁺ T_{reg} cells, and CFSE-labeled naïve Thy1.1⁺CD8⁺ OT-I T cells were adoptively transferred into naïve *Thy1.2*^{+/+} C57BL/6 mice. IV CD8⁺ T_{reg} cells were pre-treated with anti-Tim-3 antibody (or control anti-PD-L1 antibody) prior to transfer. The recipients were then SC infected with Ad-Ova and the Ig LNs were analyzed at D3. A notable reduction in the size of the draining Ig LN was observed in mice that had received IV CD8⁺ T_{reg} cells, and this was reversed with anti-Tim-3 antibody treatment (Fig. 6A). Within the draining Ig LN, IV CD8⁺ T_{reg} cells suppressed OT-I T cell division. Pre-treating IV CD8⁺ T_{reg} cells with anti-Tim-3 antibody prior to adoptive transfer restored OT-I T cell

proliferation kinetics *in vivo* comparable to animals that had received OT-I T cells alone (Fig. 6B,C). We also confirmed both IV CD8⁺ T_{reg} cells and OT-I T cells were trafficking to the T cell zone within the Ig LN by D2 (Fig. 6D). Collectively, these data imply IV CD8⁺ T_{reg} cells suppress CD8⁺ T_{eff} cell proliferation via surface Tim-3 both *in vitro* and *in vivo*.

Tim-3/HMGB-1 binding and internalization mediates CD8⁺ T_{reg} cell suppression independently of Gal-9

We next examined the mechanism for Tim-3-dependent suppression employed by liver-primed CD8⁺ T_{reg} cells. Gal-9 appeared to be uninvolved because neither rGal-9 impeded OT-I cell division nor addition of anti-Gal-9 antibody to the media of OT-I/IV CD8⁺ T_{reg} cell co-cultures reversed suppression (Fig. 7A). Tim-3 acted intrinsically on the IV CD8⁺ T_{reg} cell highlighted by anti-Tim-3 antibody pre-coating of IV CD8⁺ T_{reg} cells and lack of Tim-3 receptor expression on responder OT-I T cells (Supporting Fig. 5). HMGB-1 has been recently reported to bind Tim-3 within the early endosomes of DCs (17). These data raised the possibility that Tim-3 displayed by liver-primed CD8⁺ T_{reg} cells may bind HMGB-1 to limit T cell activation and subsequent proliferation. To test this possibility, we examined the impact of HMGB-1 blockade on OT-I T cell proliferation in culture with Ova₂₅₇₋₂₆₄ pulsed BMDCs with or without CD8⁺ T_{reg} cells. Consistent with published results, blockade of HMGB-1 diminished OT-I T cell proliferation in cultures devoid of CD8⁺ T_{reg} cells. However, in OT-I/IV CD8⁺ T cell co-cultures the expected decrease in OT-I T cell proliferation was observed, which was unaffected by HMGB-1 blockade. Thus, the CD8⁺ T_{reg} cells might suppress independently of HMGB-1 or control the concentration of HMGB-1 through a Tim-3-dependent mechanism. When we examined the contribution of Tim-3 displayed by CD8⁺ T_{reg} cells on OT-I proliferation by pre-coating the CD8⁺ T_{reg} cells with anti-Tim-3 antibody, Tim-3 blockade partially reversed CD8⁺ T_{reg} cell mediated suppression as before. Moreover, simultaneous blockade with anti-HMGB-1 and anti-Tim-3 antibodies in the co-culture restored the suppressor function of CD8⁺ T_{reg} cells (Fig. 7B). Tim-3 was indeed capable of binding HMGB-1, as rTim-3Fc chimeric protein co-immunoprecipitated with HMGB-1 present in the supernatants collected from BMDC and BMDC/OT-I cultures (Fig. 7C).

During the *in vivo* virus-induced hepatitis model where Thy1.1⁺CD8⁺ OT-I T cells were adoptively transferred into D7 Ad-Ova infected mice prior to MCMV-Ova infection, IP delivery of anti-Tim-3 antibody at D5 and D6 increased the absolute number of Thy1.1⁺CD8⁺ OT-I T cells in the livers of mice previously infected with Ad-Ova as before. Consistent with *in vitro* results, animals that received both anti-HMGB-1 and anti-Tim-3 antibodies IP failed to boost an OT-I T cell response to MCMV-Ova within the liver (Fig. 7D). These results suggest that blockade of HMGB-1 abrogates the enhancement in proliferation after Tim-3 blockade.

A histological analysis of D7 Ad-Ova infected livers revealed that the CD8⁺ T cells were exclusively sequestering HMGB-1 *in vivo* on their surface and cytoplasm (Fig. 7E). Given that DCs are a potent source of HMGB-1 within the lymph node during T cell activation, CD8⁺ T_{reg} cells may also have sequestered HMGB-1 once transferred and trafficked to the Ig LN of SC infected mice. Indeed, IV CD8⁺ T_{reg} cells bound HMGB-1 within intracellular vesicles, which co-localized with CD8⁺ T_{reg} cell Tim-3. Anti-Tim-3 antibody pre-coated IV CD8⁺ T_{reg} cells were clearly defective in internalizing HMGB-1 (Fig. 7F). In human liver biopsy specimens from chronic HCV and HCC patients, HMGB-1 was also observed to bind the surface of a subpopulation of intrahepatic CD8⁺ T cells (Fig. 8). These results describe a novel mechanism where Tim-3 on the surface of IV CD8⁺ T_{reg} cells binds HMGB-1 hampering CD8⁺ T_{eff} cell proliferation, which have a potential for translation to human liver biology.

DISCUSSION

In this report we demonstrate that hepatic viral infection results in the generation and expansion of a novel population of CD8⁺ T_{reg} cells. Regulatory activity was independent of PD-L1 expression and IL-10 production by the CD8⁺ T_{reg} cells but was dependent on Tim-3 expression. CD8⁺ T_{reg} cell Tim-3 bound HMGB-1 preventing CD8⁺ T_{eff} cell expansion. Given the role of HMGB-1 as a critical stimulus for expansion of CD8⁺ T_{eff} cells following TCR-engagement, our results suggest a novel mechanism where intrahepatic CD8⁺ T_{reg} cells limit CD8⁺ T_{eff} cell expansion via Tim-3-mediated sequestration of HMGB-1.

Previous studies have shown that liver infiltrating CD25⁺FoxP3⁺CD4⁺ T_{reg} cells dampen immune responses to hepatic viral infection (21). FoxP3⁺CD4⁺ T_{reg} cells are found in the naïve liver but do not significantly expand after adenovirus infection (data not shown). In chronic HCV infection, Tim-3 is upregulated on CD4⁺ iT_{reg} cells (22). As a result, Tim-3 binding of HMGB-1 could play a similar role on CD25⁺FoxP3⁺CD4⁺ T_{reg} cells. More research is needed to determine if CD4⁺ and CD8⁺ T_{reg} cells use Tim-3 to continuously sequester HMGB-1 released by necrotic hepatocytes and activated APCs during chronic HCV infection. This mechanism could contribute to the transition from acute to chronic infection and/or allow virus to persist during later stages of chronic disease.

The suppressive function of liver-primed CD8⁺ T_{reg} cells was exerted in an antigen-specific manner, that is recognition of peptide/MHC I complex on the APC by both the CD8⁺ T_{reg} and T_{eff} cell was necessary and sufficient for Tim-3-mediated suppression. Rangachari *et al.* establish that Tim-3 signaling is linked to TCR engagement via the Src-family kinase Lck through interaction with HLA-B-associated transcript 3 (Bat3). Gal-9 binding to Tim-3 prevented Bat-3 linkage to active Lck, thus modulating downstream TCR signaling (23). Our results support the notion that suppression of CD8⁺ T_{eff} cells is dependent on both CD8⁺ T_{reg} cell TCR recognition of antigen and Tim-3 binding to HMGB-1.

Although blockade of Tim-3 improved OT-I T cell proliferation in an HMGB-1-dependent manner, enhancement in IL-2 and IFN- γ production was only detected in the culture supernatant and was not evident on a per cell basis (data not shown). The elevated pro-inflammatory cytokine production likely reflected enhanced proliferation of responder OT-I cells. To date, HMGB-1 has been shown to improve proliferation of both CD4⁺ and CD8⁺ T cells, but enhanced levels of cytokines have only been associated with CD4⁺ T_h1 cell responses (20). It is possible that HMGB-1 only affects proliferation of CD8⁺ T_{eff} cells. Conversely, the TCR is one of the most complex signaling molecules in nature, having ten ITAM motifs, whereas most receptors utilize two. Guy *et al.* revealed that different multiplicities of ITAM and TCR signal strength uncouples proliferation and cytokine production. This effect was dependent on TCR affinity for peptide, where superagonists and strong peptides induced proliferation while weak peptides sufficiently led to maximal IL-2 secretion (24). Ovalbumin was used as the model antigen in these experiments, where the OT-I T cells receive a strong TCR signal. Since strength of signal dictates proliferation or cytokine production, we may have masked a role for Tim-3/HMGB-1 in regulating CD8⁺ T_{eff} cell cytokine production. In the future, it is worth employing another transgenic system where the responder T cells recognize a weaker peptide/MHC I complex. Alternatively, BMDCs could be pulsed with mutated ovalbumin derived peptides providing a suboptimal TCR signal.

Gal-9 and HMGB-1 are both present throughout the course of viral infection of the liver. During antiviral immune responses, including chronic HCV infection, Gal-9 is expressed by a wide variety of cells in response to elevated IFN- γ (25). Apart from activated APCs releasing HMGB-1, it can be passively released by virally lysed, cytolytically killed,

hypoxic, and oxidatively stressed hepatocytes (26). Since the binding sites for Gal-9 and HMGB-1 are distally located on Tim-3 mucin and immunoglobulin variable regions, respectively, we cannot rule out the possibility of simultaneous recognition of both ligands. In this context, the concentrations of Gal-9 and HMGB-1 along with their different avidities for Tim-3 during viral infection and cancer could balance the adaptive immune response in multiple ways. Prior research is limited because the RMT3-23 clone of anti-Tim-3 antibody is effective at blocking both Gal-9 and HMGB-1 binding to Tim-3 (17,27).

Approximately 600 million people worldwide are in danger of developing chronic liver disease due to HBV/HCV, and only a subset of these patients respond to IFN- α /ribavirin therapy (3). Simultaneous blockade of the IL-10, PD-1/PD-L1, and Tim-3 inhibitory pathways has potential clinical efficacy. However, elevated serum HMGB-1 during HCV infection directly correlates with liver disease progression (28). HMGB-1 sequestration by T_{reg} cell Tim-3 may therefore not be sufficient to suppress T_{eff} cells under conditions of extensive liver injury and HMGB-1 release. We herein report that HMGB-1 staining co-localizes to the surface of CD8⁺ T cell subpopulations found in chronic HCV and HCC liver biopsies; therefore, a role for HMGB-1 in advanced human diseases remains to be elucidated. Thus, disease progression, signaling pathway integration, and ligand concentration, accessibility, and avidity for receptors must all be considered in the design of immunotherapeutic strategies.

In summary, these data describe a novel mechanism where Tim-3 binds HMGB-1 on virus-specific CD8⁺ T_{reg} cells suppressing the proliferation of CD8⁺ T_{eff} cells during acute adenovirus infection. This observation provides a framework for future studies of Tim-3, where consideration for ligand access of both Gal-9 and HMGB-1 is warranted. Translation to human liver disease is expected given that a similar population of IL-10-producing, PD-1/PD-L1⁺Tim-3⁺CD8⁺ T cells exists in liver biopsies of chronic HCV patients.

Supplementary Material

Refer to Web version on PubMed Central for supplementary material.

Acknowledgments

Financial Support

NIH Grants DK063222, U19 AI083024, and Immunology Training Fellowship T32 AI07496 supported this publication.

After pilot experiments established a CD8⁺ T_{reg} cell phenotype, Jie Sun at Indiana University kindly aided in optimizing CD8⁺ T cell co-culture experiments. We also thank Taeg Kim and Hai-Chon Lee of the University of Virginia for their contributions in experimental design. Sun-Sang Sung and the University of Virginia Advanced Microscopy Facility assisted in confocal imaging. Michael Solga and the University of Virginia Flow Cytometry Core Facility contributed to performing and outlining FACS-sorting experiments.

List of Abbreviations

Ad	adenovirus
ALT	alanine aminotransferase
APC	antigen presenting cell
BMDC	bone marrow-derived dendritic cell
C LN	celiac lymph node

D	day
DAMP	danger associated molecular pattern
DC	dendritic cell
FMO	fluorescence minus one
Gal-9	galectin-9
GrB	granzyme B
HBV	hepatitis B virus
HCC	hepatocellular carcinoma
HCV	hepatitis C virus
HMGB-1	high-mobility group box 1
Ig LN	inguinal lymph node
IP	intraperitoneal
IV	intravenous
MCMV	mouse cytomegalovirus
PAMP	pathogen associated molecular pattern
PD-1	programmed death 1
PD-L1	PD-1 ligand
PLP	periodate-lysine-paraformaldehyde fixative
RAGE	receptor for advanced glycation end products
SC	subcutaneous
TCR	T cell receptor
T_{eff}	T effector
Tim-3	T cell immunoglobulin and mucin 3
T_{reg}	T regulatory

References

1. Crispe IN. The Liver as a Lymphoid Organ. *Annu Rev Immunol.* 2009; 27:147–163. [PubMed: 19302037]
2. Lukens JR, Dolina JS, Kim TS, Tacke RS, Hahn YS. Liver is able to activate naïve CD8+ T cells with dysfunctional anti-viral activity in the murine system. *PLoS ONE.* 2009; 4:e7619. [PubMed: 19876399]
3. Callendret B, Walker C. A siege of hepatitis: Immune boost for viral hepatitis. *Nat Med.* 2011; 17:252–253. [PubMed: 21383718]
4. Tiegs G, Lohse AW. Immune tolerance: What is unique about the liver. *Journal of Autoimmunity.* 2010; 34:1–6. [PubMed: 19717280]
5. Mills KHG. Regulatory T cells: friend or foe in immunity to infection? *Nat Rev Immunol.* 2004; 4:841–855. [PubMed: 15516964]
6. Takahashi T, Tagami T, Yamazaki S, Uede T, Shimizu J, Sakaguchi N, et al. Immunologic self-tolerance maintained by CD25(+)CD4(+) regulatory T cells constitutively expressing cytotoxic T lymphocyte-associated antigen 4. *J Exp Med.* 2000; 192:303–310. [PubMed: 10899917]

7. Strauss L, Bergmann C, Whiteside TL. Human circulating CD4⁺CD25^{high}Foxp3⁺ regulatory T cells kill autologous CD8⁺ but not CD4⁺ responder cells by Fas-mediated apoptosis. *The Journal of Immunology*. 2009; 182:1469–1480. [PubMed: 19155494]
8. Kim H-J, Wang X, Radfar S, Sproule TJ, Roopenian DC, Cantor H. CD8⁺ T regulatory cells express the Ly49 Class I MHC receptor and are defective in autoimmune prone B6-Yaa mice. *Proc Natl Acad Sci USA*. 2011; 108:2010–2015. [PubMed: 21233417]
9. Salti SM, Hammelev EM, Grewal JL, Reddy ST, Zemple SJ, Grossman WJ, et al. Granzyme B Regulates Antiviral CD8⁺ T Cell Responses. *The Journal of Immunology*. 2011; 187:6301–6309. [PubMed: 22084442]
10. Kitazawa Y, Fujino M, Wang Q, Kimura H, Azuma M, Kubo M, et al. Involvement of the Programmed Death-1/Programmed Death-1 Ligand Pathway in CD4⁺CD25⁺ Regulatory T-Cell Activity to Suppress Alloimmune Responses. *Transplantation*. 2007; 83:774–782. [PubMed: 17414712]
11. Blackburn SD, Wherry EJ. IL-10, T cell exhaustion and viral persistence. *Trends Microbiol*. 2007; 15:143–146. [PubMed: 17336072]
12. Jin H-T, Anderson AC, Tan WG, West EE, Ha S-J, Araki K, et al. Cooperation of Tim-3 and PD-1 in CD8 T-cell exhaustion during chronic viral infection. *Proc Natl Acad Sci USA*. 2010; 107:14733–14738. [PubMed: 20679213]
13. Couper KN, Blount DG, Riley EM. IL-10: the master regulator of immunity to infection. *J Immunol*. 2008; 180:5771–5777. [PubMed: 18424693]
14. Fife BT, Pauken KE, Eagar TN, Obu T, Wu J, Tang Q, et al. Interactions between PD-1 and PD-L1 promote tolerance by blocking the TCR-induced stop signal. *Nat Immunol*. 2009; 10:1185–1192. [PubMed: 19783989]
15. Golden-Mason L, Palmer BE, Kassam N, Townshend-Bulson L, Livingston S, McMahon BJ, et al. Negative Immune Regulator Tim-3 Is Overexpressed on T Cells in Hepatitis C Virus Infection and Its Blockade Rescues Dysfunctional CD4⁺ and CD8⁺ T Cells. *Journal of Virology*. 2009; 83:9122–9130. [PubMed: 19587053]
16. Cao E, Zang X, Ramagopal UA, Mukhopadhyaya A, Fedorov A, Fedorov E, et al. T Cell Immunoglobulin Mucin-3 Crystal Structure Reveals a Galectin-9-Independent Ligand-Binding Surface. *Immunity*. 2007; 26:311–321. [PubMed: 17363302]
17. Chiba S, Baghdadi M, Akiba H, Yoshiyama H, Kinoshita I, Dosaka-Akita H, et al. Tumor-infiltrating DCs suppress nucleic acid-mediated innate immune responses through interactions between the receptor TIM-3 and the alarmin HMGB1. *Nature Publishing Group*. 2012; 13:832–842.
18. Lotze MT, Tracey KJ. High-mobility group box 1 protein (HMGB1): nuclear weapon in the immune arsenal. *Nat Rev Immunol*. 2005; 5:331–342. [PubMed: 15803152]
19. Dumitriu IE, Baruah P, Valentini B, Voll RE, Herrmann M, Nawroth PP, et al. Release of high mobility group box 1 by dendritic cells controls T cell activation via the receptor for advanced glycation end products. *J Immunol*. 2005; 174:7506–7515. [PubMed: 15944249]
20. Sundberg E, Fasth AER, Palmblad K, Harris HE, Andersson U. High mobility group box chromosomal protein 1 acts as a proliferation signal for activated T lymphocytes. *Immunobiology*. 2009; 214:303–309. [PubMed: 19201506]
21. Xu D, Fu J, Jin L, Zhang H, Zhou C, Zou Z, et al. Circulating and liver resident CD4⁺CD25⁺ regulatory T cells actively influence the antiviral immune response and disease progression in patients with hepatitis B. *J Immunol*. 2006; 177:739–747. [PubMed: 16785573]
22. Moorman JP, Wang JM, Zhang Y, Ji XJ, Ma CJ, Wu XY, et al. Tim-3 Pathway Controls Regulatory and Effector T Cell Balance during Hepatitis C Virus Infection. *The Journal of Immunology*. 2012
23. Rangachari M, Zhu C, Sakuishi K, Xiao S, Karman J, Chen A, et al. Bat3 promotes T cell responses and autoimmunity by repressing Tim-3-mediated cell death and exhaustion. *Nat Med*. 2012; 18:1394–1400. [PubMed: 22863785]
24. Guy CS, Vignali KM, Temirov J, Bettini ML, Overacre AE, Smeltzer M, et al. Distinct TCR signaling pathways drive proliferation and cytokine production in T cells. *Nature Publishing Group*. 2013; 14:262–270.

25. Rodriguez-Manzanet R, DeKruyff R, Kuchroo VK, Umetsu DT. The costimulatory role of TIM molecules. *Immunol Rev.* 2009; 229:259–270. [PubMed: 19426227]
26. Klune J, Dhupar R. HMGB1: Endogenous Danger Signaling. *Mol Med.* 2008; 14:1.
27. Kanzaki M, Wada J, Sugiyama K, Nakatsuka A, Teshigawara S, Murakami K, et al. Galectin-9 and T Cell Immunoglobulin Mucin-3 Pathway Is a Therapeutic Target for Type 1 Diabetes. *Endocrinology.* 2012; 153:612–620. [PubMed: 22186414]
28. Jung JH, Park JH, Jee MH, Keum SJ, Cho MS, Yoon SK, et al. Hepatitis C Virus Infection Is Blocked by HMGB1 Released from Virus-Infected Cells. *Journal of Virology.* 2011; 85:9359–9368. [PubMed: 21752923]

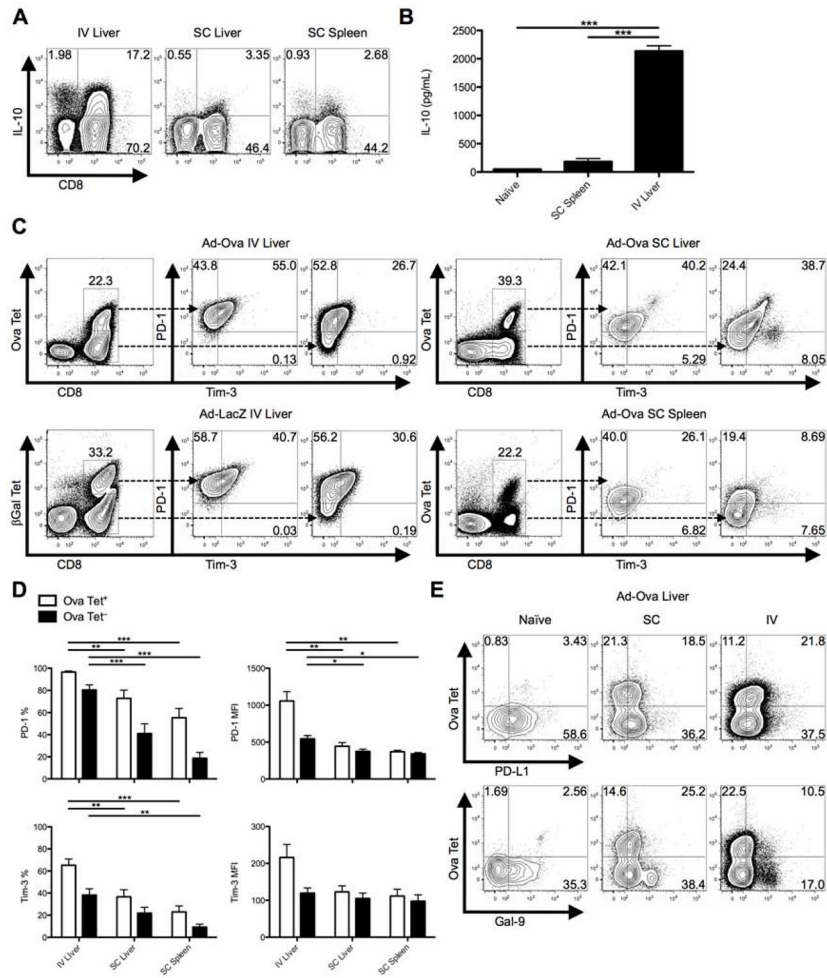


Fig. 1. IL10, PD-1, and Tim-3 are co-expressed on liver-primed CD8⁺ T cells after IV adenovirus infection

C57BL/6 mice were SC or IV infected with 2.5×10^7 IU Ad-Ova. (A) Endogenous D7 liver and spleen T cell IL-10 production was assessed after a 5 hr re-stimulation with 5 ng/mL PMA and 500 ng/mL ionomycin ($n = 3$ per group). (B) CD8⁺ T cells sorted from naïve liver, D7 SC spleen, and D7 IV liver were re-stimulated *in vitro* with plate-bound anti-CD3 ϵ Ab and soluble anti-CD28 Ab. The concentration of IL-10 was measured in the D2 culture supernatant by ELISA (one-way ANOVA/Tukey's post test; $n = 3$ per group). (C and D) Co-expression of PD-1 and Tim-3 was determined directly *ex vivo* for Ova Tet⁺ and Ova Tet⁻ populations of CD8⁺ T cells at D7 post-infection. Ad-Ova IV infection in the liver was also compared to D7 livers from Ad-LacZ IV infected C57BL/6 mice (one-way ANOVA/Tukey's post test; $n = 4-9$ per group). (E) PD-L1 and Gal-9 ligand expression was characterized in livers of naïve, SC, and IV Ad-Ova infected animals ($n = 3-6$ per group). Numbers in the scatter plots represent percentages. Mean \pm s.e.m.; * $P < 0.05$, ** $P < 0.01$, and *** $P < 0.001$.

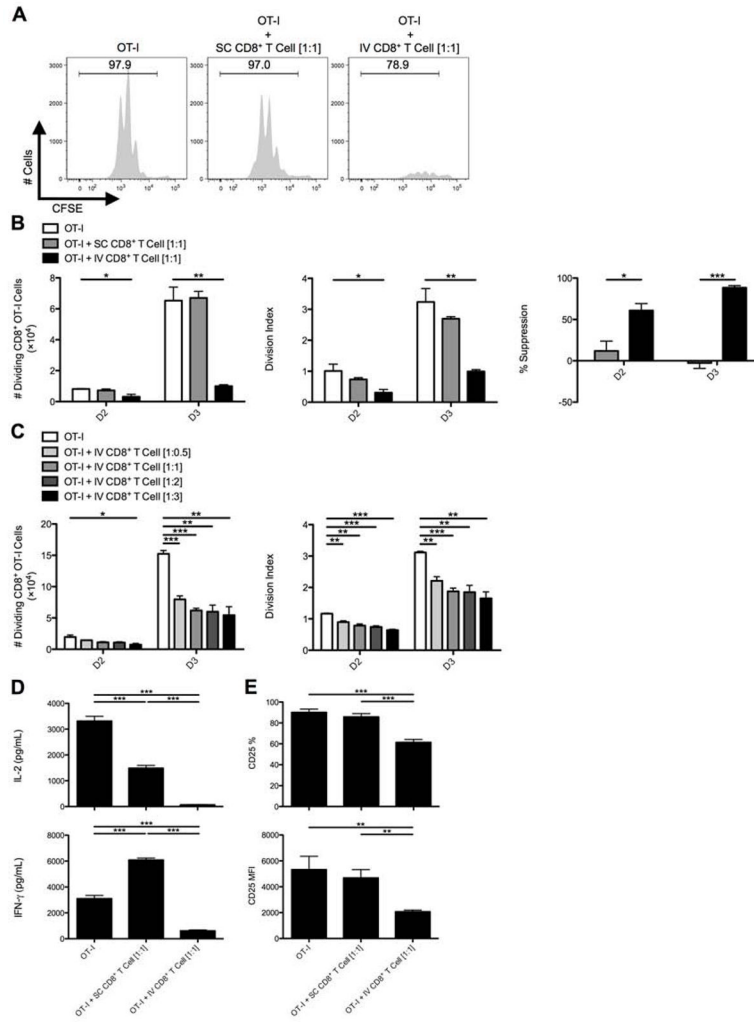


Fig. 2. CD8⁺ T cells from the livers of IV infected animals suppress the activation and expansion of naïve CD8⁺ OT-I T cells *in vitro*

C57BL/6 mice were SC or IV infected with 2.5×10^7 IU Ad-Ova, and (A) bulk CD8⁺ T cells were isolated from D7 SC spleens and IV livers then cultured with CFSE-labeled naïve Thy1.1⁺CD8⁺ OT-I T cells at a 1:1 ratio. SIINFEKL-pulsed BMDCs were used as the source of antigen, and co-cultures were analyzed at D3. (B) The number of dividing OT-I T cells, OT-I T cell division index, and percent suppression displayed by either SC CD8⁺ T cells or IV CD8⁺ T cells was calculated at D2 and D3 of culture (one-way ANOVA/Tukey's post test; n = 12 per group). (C) Naïve Thy1.1⁺CD8⁺ OT-I T cells were also cultured at various ratios relative to CD8⁺ T cells collected from the livers of IV infected mice (1:0.5, 1:1, 1:2, and 1:3) (one-way ANOVA/Tukey's post test; n = 3 per group). (D) The concentrations of IL-2 and IFN-γ were measured in the D3 culture supernatants by ELISA, and (E) CD25 expression was determined directly *ex vivo* on D3 Thy1.1⁺CD8⁺ OT-I T cells (one-way ANOVA/Tukey's post test; n = 5–6 per group). Numbers in the histograms represent percentages. Mean ± s.e.m.; **P* < 0.05, ***P* < 0.01, and ****P* < 0.001.

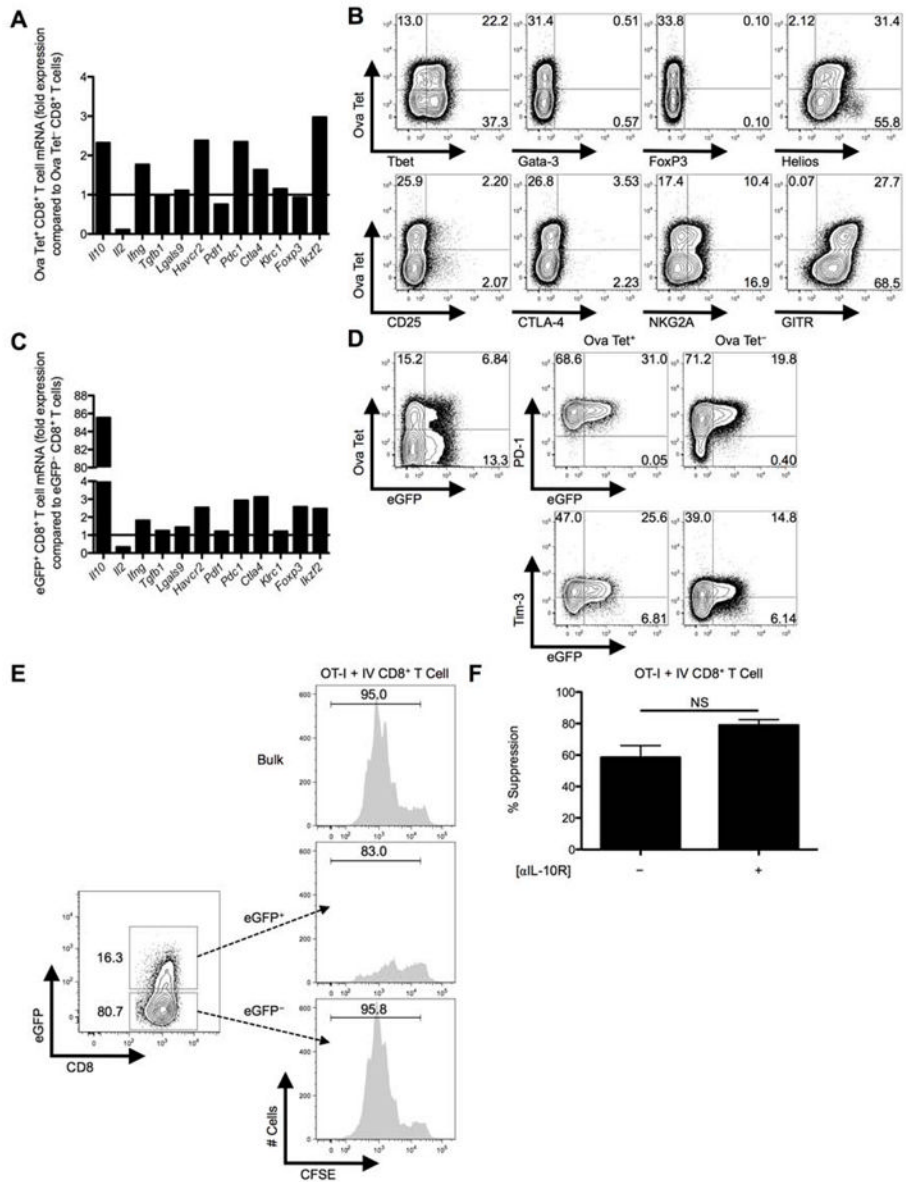


Fig. 3. eGFP⁺CD8⁺ T_{reg} cells are more potent suppressors compared to eGFP⁻CD8⁺ T_{reg} cells from IL-10 transcriptional reporter mice and display some canonical T_{reg} markers
 C57BL/6 mice were IV infected with 2.5×10^7 IU Ad-Ova, D7 liver mononuclear cells were isolated, and total RNA was collected from FACS-sorted Ova Tet⁺ and Ova Tet⁻CD8⁺ T_{reg} cells. (A) *Il10* (IL-10), *Il2* (IL-2), *Ifng* (IFN- γ), *Tgfb* (TGF- β), *Lgals9* (Gal-9), *Havcr2* (Tim-3), *Pdli* (PD-L1), *Pdcl* (PD-1), *Ctla4* (CTLA-4), *Klrc1* (NKG2A), *Foxp3* (FoxP3), and *Ilkzf2* (Helios) mRNA was measured by Q-PCR. (B) Expression of intranuclear/cellular Tbet/Gata-3/FoxP3/Helios, and surface CD25/CTLA-4/NKG2A/GITR was determined on CD8⁺ T_{reg} cells from the livers of IV infected mice. (C) Similarly, transcript from FACS-sorted eGFP⁺CD8⁺ T_{reg} cells was compared to that of eGFP⁻CD8⁺ T_{reg} cells from D7 IV infected Vert-X mice. (D) PD-1 and Tim-3 surface expression along the eGFP profile was separately assessed on Ova Tet⁺ and Ova Tet⁻CD8⁺ T_{reg} cells (n = 3 per group). (E) Representative *in vitro* suppression assays from bulk CD8⁺ T_{reg} cells and FACS-sorted eGFP⁺CD8⁺ T_{reg} cells or eGFP⁻CD8⁺ T_{reg} cells from D7 Ad-Ova IV infected C57BL/6 and Vert-X mice, respectively, co-cultured with CFSE-labeled naïve Thy1.1⁺CD8⁺ OT-I T cells

at a 1:1 ratio are depicted (n = 3 per group). (F) D3 percent suppression by D7 Ad-Ova liver-primed CD8⁺ T_{reg} cells during co-culture with CFSE-labeled naïve Thy1.1⁺CD8⁺ OT-I T cells at a 1:1 ratio and SIINKFEKL-pulsed BMDCs is displayed. Select wells also contained anti-IL-10R Ab in the media during culture (n = 3 per group). Numbers in the histograms and scatter plots represent percentages.

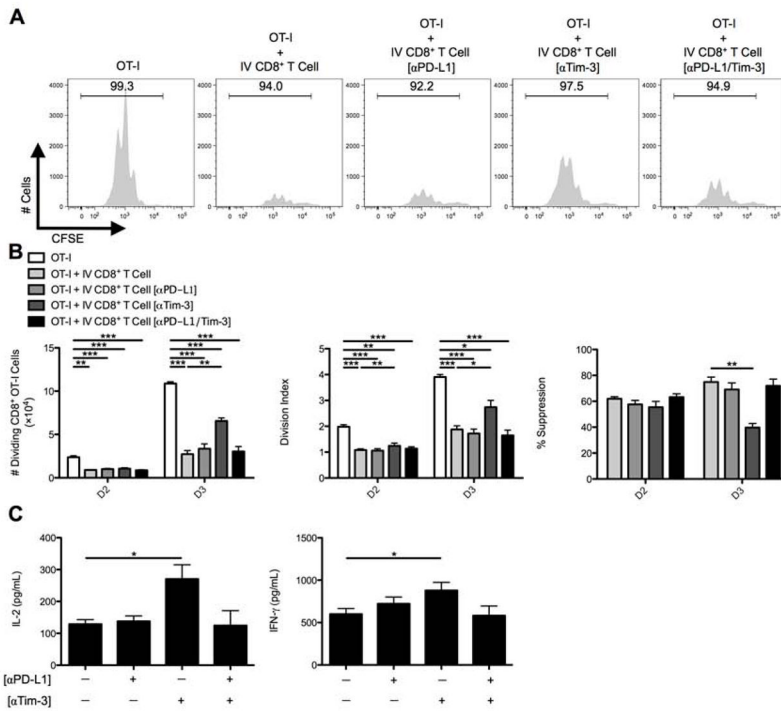


Fig. 4. *In vitro* CD8⁺ T_{reg} cell suppression is dictated by the Tim-3 inhibitory pathway C57BL/6 mice were IV infected with 2.5×10⁷ IU Ad-Ova, and (A) bulk CD8⁺ T_{reg} cells were isolated from D7 IV livers. Before co-culture with CFSE-labeled naïve Thy1.1⁺CD8⁺ OT-I T cells at a 1:1 ratio and SIINKFEKL-pulsed BMDCs, the CD8⁺ T_{reg} cells were left alone or pre-coated with anti-PD-L1 Ab, anti-Tim-3 Ab, or both. Cell cultures were analyzed at D3 for CFSE dilution. (B) The number of dividing OT-I T cells, OT-I T cell division index, and percent suppression displayed by IV CD8⁺ T_{reg} cells was calculated at D2 and D3 of culture. (C) The concentrations of IL-2 and IFN-γ were measured in the D3 culture supernatants by ELISA (one-way ANOVA/Tukey’s post test; n = 6–9 per group). Numbers in the histograms represent percentages. Mean ± s.e.m.; *P < 0.05, **P < 0.01, and ***P < 0.001.

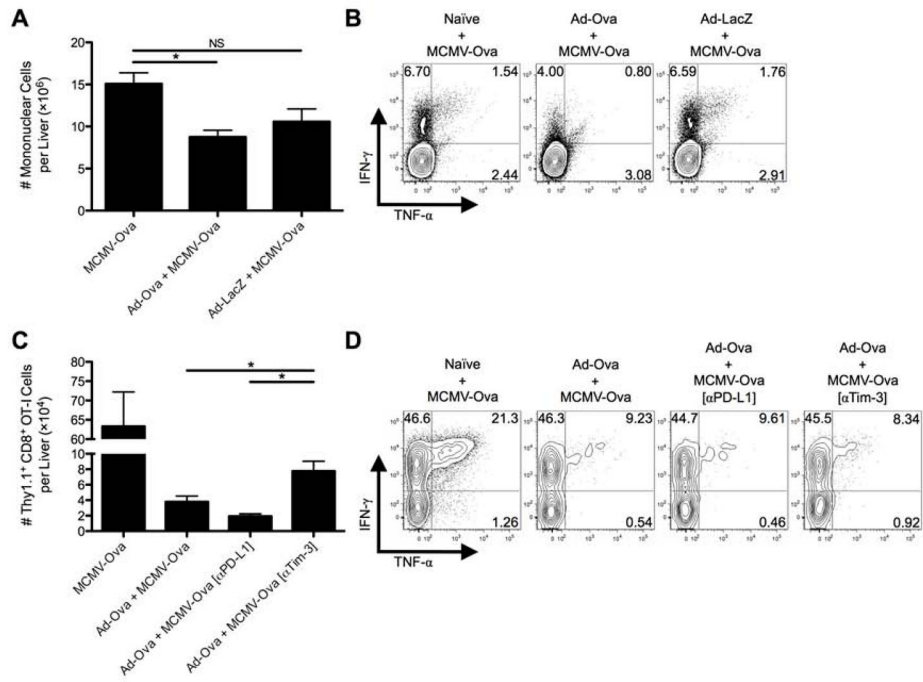


Fig. 5. Tim-3 blockade improves antigen-specific hepatic secondary immune responses to viral infection
 C57BL/6 mice were IV infected with 2.5×10^7 IU Ad-Ova, 2.5×10^7 IU Ad-LacZ, or left uninfected. At D7, all 3 experimental groups were IV infected with 1×10^4 IU MCMV-Ova. (A) The number of live mononuclear cells isolated from the livers of D14 infected animals was enumerated. Trypan blue exclusion was used to assess the number of viable cells. (B) Endogenous CD8⁺ T cell TNF- α and IFN- γ were quantified at D14 after a 5 hr re-stimulation with 2 μ g/mL SIINFEKL peptide (n = 3 per group). (C and D) In a parallel experiment, 5×10^5 naïve Thy1.1⁺CD8⁺ OT-I T cells were transferred at D7. C57BL/6 mice were left untreated or were administered 300 μ g anti-PD-L1 Ab or anti-Tim-3 Ab IP at D5 and D6 prior to a D7 MCMV-Ova infection. The number of Thy1.1⁺CD8⁺ OT-I T cells and their TNF- α and IFN- γ production was assessed in the livers of infected animals at D14. Cytokine detection was achieved after a 5 hr re-stimulation with 2 μ g/mL SIINFEKL peptide (one-way ANOVA/Tukey's post test; n = 3 per group). Numbers in the scatter plots represent percentages. Mean \pm s.e.m.; * $P < 0.05$.

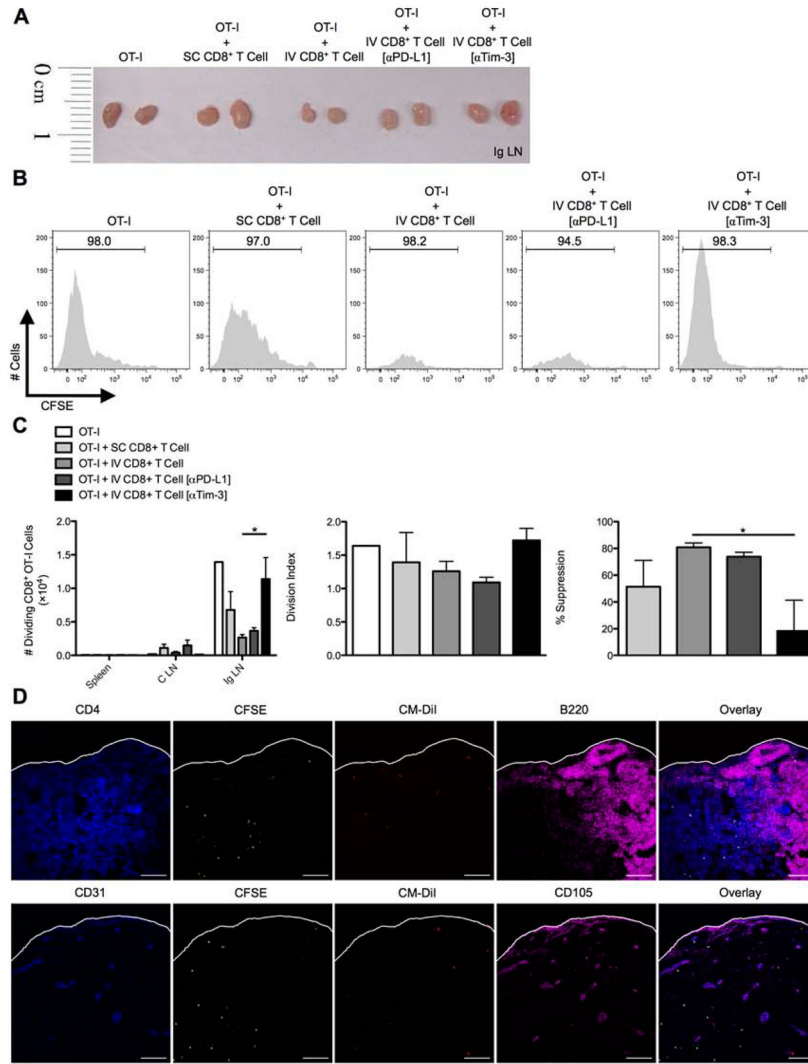


Fig. 6. *In vivo* CD8⁺ T_{reg} cell suppression of SC-primed OT-I cells entering draining lymph nodes is regulated by Tim-3

C57BL/6 mice were SC or IV infected with 2.5×10^7 IU Ad-Ova, and bulk CD8⁺ T cells were isolated from D7 SC spleens and IV livers. D7 CD8⁺ T_{reg} cells from IV infected livers were left alone or pre-coated with anti-PD-L1 Ab or anti-Tim-3 Ab. CFSE-labeled naïve Thy1.1⁺CD8⁺ OT-I T cells were adoptively transferred alone or in combination with CD8⁺ T cells from infected spleens and livers at a 1:2 ratio, respectively, into naïve C57BL/6 mice. Shortly thereafter, these recipient mice were SC infected. At D3 post-infection, the spleens, celiac lymph nodes (C LN), and (A and B) inguinal lymph nodes (Ig LN) were harvested, and (C) the number of dividing OT-I T cells was determined in each organ. The division index and percent suppression of OT-I T cells in the Ig LN is displayed (one-way ANOVA/Tukey's post test; n = 3–6 per group). (D) CM-DiI-labeled CD8⁺ T_{reg} cells from D7 IV infected liver (red) and CFSE-labeled naïve Thy1.1⁺CD8⁺ OT-I T cells (green) were transferred in a similar experiment and Ig LNs were harvested at D2 SC post-infection. PLP-fixed/OCT-frozen Ig LN cross sections were stained with anti-CD4 (blue-upper panel), anti-CD31 (blue-lower panel), anti-B220 (magenta-upper panel), and CD105 (magenta-lower panel) (n = 3 per group). Scale bar, 100 μm. Numbers in the histograms represent percentages. Mean ± s.e.m.; *P < 0.05.

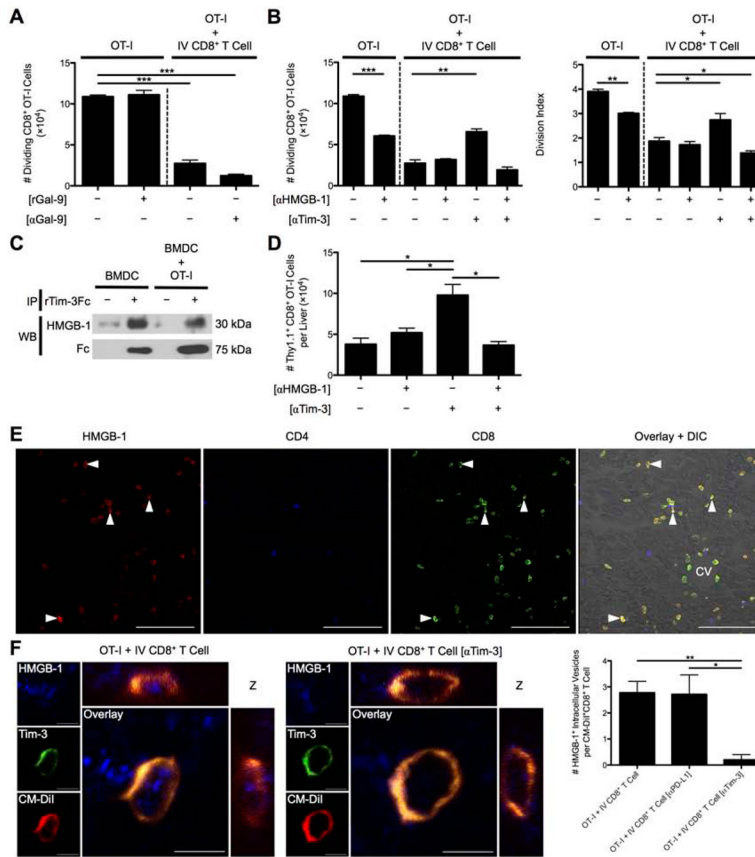


Fig. 7. Tim-3 binding to HMGB-1 controls CD8⁺ T_{reg} cell suppression independently of Gal-9
 (A) The number of dividing OT-I T cells at D3 was determined when rGal-9 was included in the media of CFSE-labeled naïve Thy1.1⁺CD8⁺ OT-I T cells cultured with SIINFEKL-pulsed BMDCs and when these cells were co-cultured with D7 Ad-Ova liver-primed CD8⁺ T_{reg} cells in the presence of anti-Gal-9 Ab (n = 3 per group). (B) D7 Ad-Ova primed CD8⁺ T_{reg} cells were isolated from livers, left alone or pre-coated with anti-Tim-3 Ab, and co-cultured with CFSE-labeled naïve Thy1.1⁺CD8⁺ OT-I T cells at a 1:1 ratio and SIINFEKL-pulsed BMDCs. Select wells also contained anti-HMGB-1 Ab in the media during culture. D3 CFSE dilution and number of dividing OT-I T cells and OT-I T cell division index were evaluated (one-way ANOVA/Tukey's post test; n = 6 per group). (C) Supernatants from media obtained from BMDCs maturing in the presence of rIL-4 and rGM-CSF and from D1 BMDC co-culture with OT-I T cells were incubated with rTim-3Fc chimeric protein for 1 hr, followed by immunoprecipitation with protein A/G and immunoblot analysis with anti-HMGB-1 Ab or anti-human Fc (n = 3 per group). (D) 5 × 10⁵ naïve Thy1.1⁺CD8⁺ OT-I T cells were transferred into D7 Ad-Ova infected mice, which were left untreated or received 300 µg anti-HMGB-1 Ab or anti-Tim-3 Ab IP at D5 and D6 prior to a D7 MCMV-Ova infection. The number of Thy1.1⁺CD8⁺ OT-I T cells was assessed in the livers of infected animals at D14 (one-way ANOVA/Tukey's post test; n = 3–6 per group). (E) PLP-fixed/OCT-frozen liver cross sections from D7 livers were stained with anti-HMGB-1 (red), anti-CD4 (blue), and anti-CD8 (green). Central vein (CV) is indicated (n = 6 per group). Scale bar, 100 µm. (F) 3D orthogonal view representative of PLP-fixed/OCT-frozen Ig LN cross sections from C57BL/6 mice that received CM-DiI-labeled CD8⁺ T_{reg} cells from D7 infected liver (red) and CFSE-labeled naïve Thy1.1⁺CD8⁺ OT-I T cells stained with anti-HMGB-1 (blue) and anti-Tim-3 (green) is shown. Scale bar, 5 µm. Quantification of intracellular HMGB-1⁺ perinuclear vesicles within uncoated, anti-PD-

L1 Ab pre-coated, and anti-Tim-3 Ab pre-coated CD8⁺ T_{reg} cells was assessed per cell in images (one-way ANOVA/Tukey's post test; n = 3 per group). Numbers in the histograms represent percentages. Mean \pm s.e.m.; * P < 0.05, ** P < 0.01, and *** P < 0.001.

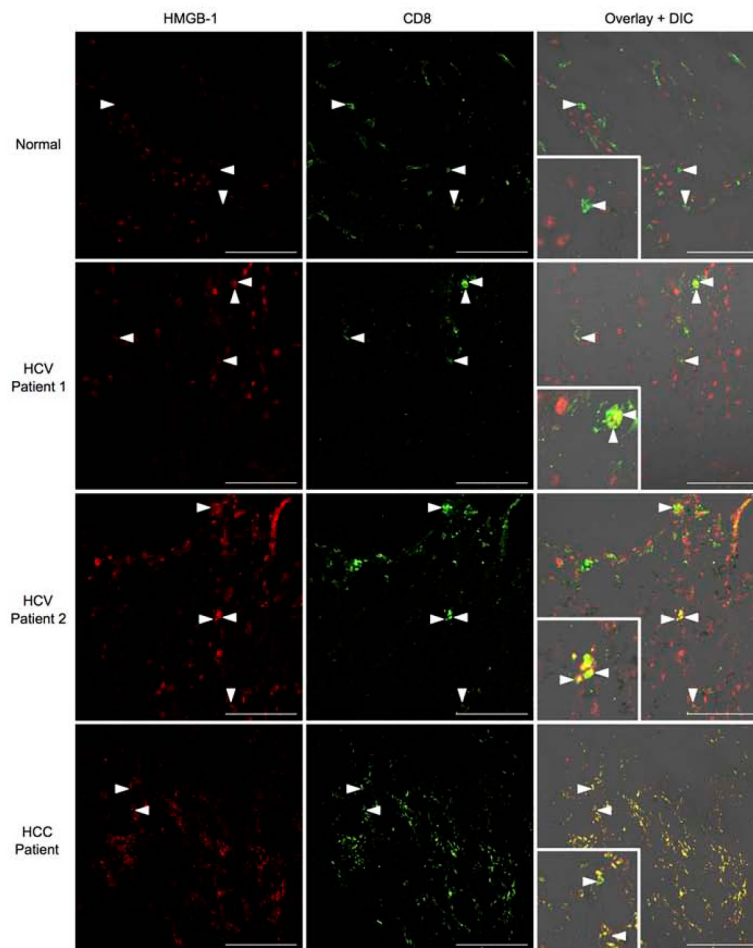


Fig. 8. HMGB-1 binds to CD8⁺ T cells in the livers of chronic HCV and HCC patients
 Acetone-fixed liver cross sections of human biopsies from normal donors, chronic HCV patients, and HCC patients were stained with anti-HMGB-1 (red) and anti-CD8 (green). The inlays depict areas of HMGB-1/CD8 co-localization in HCC/HCV patients (Normal n = 3 per group; HCV n = 5 per group; HCC n = 2 per group). Representative images are displayed. Scale bar, 100 μ m.